Geomechanics and Engineering, *Vol. 36, No. 6 (2024) 601-618*
https://doi.org/10.12989/gae.2024.36.6.601

A Copula method for modeling the intensity characteristic of geotechnical strata of roof based on small sample test data

Jiazeng Cao[1,2,3,4], Tao Wang*[1,2,3,4], Mao Sheng[2], Yingying Huang[3] and Guoqing Zhou[1]

[1]*State Key Laboratory for Geomechanics and Deep Underground Engineering, School of Mechanics and Civil Engineering, China University of Mining and Technology, Xuzhou, Jiangsu, 221116, China*
[2]*National Key Laboratory of Petroleum Resources and Engineering, China University of Petroleum, Beijing 102249, China*
[3]*Key Laboratory of Geohazard Prevention of Hilly Mountains, Ministry of Natural Resources, Fujian Key Laboratory of Geohazard Prevention, Fuzhou, Fujian 350002, China*
[4]*Technology Innovation Center for Mine Geological Environment Restoration in the Alpine and Arid Regions, MNR, Lanzhou, Gansu, 730000, China*

(*Received January 12, 2023, Revised February 13, 2024, Accepted March 2, 2024*)

Abstract. The joint probability distribution of uncertain geomechanical parameters of geotechnical strata is a crucial aspect in constructing the reliability functional function for roof structures. However, due to the limited number of on-site exploration and test data samples, it is challenging to conduct a scientifically reliable analysis of roof geotechnical strata. This study proposes a Copula method based on small sample exploration and test data to construct the intensity characteristics of roof geotechnical strata. Firstly, the theory of multidimensional copula is systematically introduced, especially the construction of four-dimensional Gaussian copula. Secondly, data from measurements of 176 groups of geomechanical parameters of roof geotechnical strata in 31 coal mines in China are collected. The goodness of fit and simulation error of the four-dimensional Gaussian Copula constructed using the Pearson method, Kendall method, and Spearman methods are analyzed. Finally, the fitting effects of positive and negative correlation coefficients under different copula functions are discussed respectively. The results demonstrate that the established multidimensional Gaussian Copula joint distribution model can scientifically represent the uncertainty of geomechanical parameters in roof geotechnical strata. It provides an important theoretical basis for the study of reliability functional functions for roof structures. Different construction methods for multidimensional Gaussian Copula yield varying simulation effects. The Kendall method exhibits the best fit in constructing correlations of geotechnical parameters. For the bivariate Copula fitting ability of uncertain parameters in roof geotechnical strata, when the correlation is strong, Gaussian Copula demonstrates the best fit, and other Copula functions also show remarkable fitting ability in the region of fixed correlation parameters. The research results can offer valuable reference for the stability analysis of roof geotechnical engineering.

Keywords: coal seam roof; Gaussian copula; joint probability distribution; small sample; uncertain mechanical parameters

1. Introduction

In coal mine geotechnical engineering, due to the limitations of mining geological environment and exploration testing conditions, the test data for the rock and soil parameters of the coal seam roof are often very limited, and the statistical characteristics exhibit significant variability and uncertainty. Consequently, evaluating the reliability of the coal seam roof's rock and soil layers is highly challenging. To accurately analyze the stability of coal mine geotechnical engineering, it is typically necessary to obtain comprehensive probabilistic information, which involves acquiring the joint probability distribution of the required parameters. Only through obtaining this joint probability distribution can a scientifically reliable functional function be constructed for the stability analysis. However, under the condition of small sample or even missing survey data (Phoon 2020), the measured data with large variability cannot truly describe the real marginal distribution and correlation structure of coal mine mechanical parameters, thus the joint probability density distribution model cannot be further determined. Copula method has been continuously used and developed in the field of finance and hydrology (Embraechts *et al.* 1999, Nelson 2006, Palaro *et al.* 2006, Salvadori and Michele 2007). It provides an effective method for solving the joint probability distribution of mechanical parameters. The joint probability distribution of parameters is converted into marginal distribution function between parameters and to select the Copula function connecting these parameters. A joint probability distribution of uncertain geotechnical parameters can be constructed by this method.

In the past decade, the application of copula theory to reliability analysis research in geotechnical engineering has been relatively rare. Huffman and Stuedlein (2014) constructed the joint distribution of load-displacement power-law curve parameters based on bivariate copula, and

*Corresponding author, Ph.D.
E-mail: taowang@cumt.edu.cn

ISSN: 2005-307X (Print), 2092-6219 (Online)

then proposed an empirical formula for calculating the load resistance coefficient of reinforced clay strip foundation. By constructing the joint probability distribution function of shear mechanical parameters of vegetation slope and establishing the dependence structure of c and φ via copula theory, Das *et al.* (2018) revealed that the slope stability increases significantly with the increase of correlation. Prakash *et al.* (2019) used multidimensional Gaussian copula to analyze the density distribution function of soil-water characteristic curve, and evaluated the stability of unsaturated slopes. Based on copula entropy and mutual information theory, Zheng *et al.* (2018) constructed a new factor selection method, established a complete high dam monitoring and uncertainty integration method system, which improved the prediction accuracy in actual monitoring projects. Ng *et al.* (2021) develops a new method to generate copula-based rotated anisotropy random fields for characterizing the spatial variability of soil properties, and suggestions for potential failure of slope are given for both failure probability and failure consequence.

At present, the research on parameter uncertainty is developing in structural engineering (Soumya *et al.* 2015, Minh and Jun 2021) and geotechnical engineering (Bulent 2017, Ramanandan and Dodagoudar 2020) on the basis of deterministic analysis of mechanical parameters(Wang *et al*. 2022, Zhang *et al*. 2022, Hosseini *et al*. 2023). The jointly distributed random variables method can be used to solve the problem of probability evaluation and engineering reliability analysis. Johari *et al.* (2013) used the joint distribution random variable method, and regarded the density, elastic modulus and Poisson 's ratio as random parameters to perform probability analysis and reliability evaluation on the shear wave velocity relationship. In the prediction of liquefaction potential, Johari *et al.* (2012) used the joint distribution random variable method for probability analysis and reliability evaluation of liquefaction potential. In the reliability analysis of rock slope stability, the joint distribution random variable method is used to obtain that the friction angle of the sliding surface is the most effective parameter in the stability of the plane sliding rock slope. (Johari *et al*. 2015). In geotechnical engineering, most of the current engineering application research based on copula theory focuses on slope reliability research (Li *et al.* 2010, Tang *et al.* 2020).

The research on correlated non-normal variables also focuses on the impact of negative correlation on engineering decision-making (Phoon *et al.* 2010). There are few researches on the correlation parameters of coal mine geotechnical engineering, especially based on the background of small sample investigation and testing. In the study of the stability of coal mine roof, the parameters are often regarded as deterministic variables (Sherizadeh and Kulatilake 2016, Lukasz and Tadeusz 2020, Kong *et al*. 2021, Zhang *et al.* 2021). At the same time, the stability of geotechnical structure is often not caused by a single factor, which needs to consider the correlation between multiple parameters. Therefore, it is very essential to study the joint probability distribution of uncertain mechanical parameters of coal seam roof under small sample test data.

This study proposes a Copula method based on small sample exploration and test data to construct the intensity characteristics of roof geotechnical strata. The Copula theory is systematically introduced and the construction method of multidimensional Gaussian Copula is provided. Based on small sample measured data, the goodness of fit and simulation error of the four-dimensional Gaussian Copula constructed using the Pearson method, Kendall method, and Spearman methods are analyzed. The influence of different Copula function structures on the fitting ability of the original data is discussed. The results can provides an important theoretical basis for the study of reliability functional functions for roof structures.

2. Construction method

2.1 Copula theory

Sklar (1959) proposed the Copula method. The joint probability distribution of parameters is converted into marginal distribution function between parameters and to select the Copula function connecting these parameters. It can be simply summarized as follows

$$G(x_1,x_2,\cdots,x_n)=C\left(F_1(x_1),F_2(x_2),\cdots,F_n(x_n)\right)=C(u_1,u_2,\cdots u_n) \quad (1)$$

where $G(x_1, x_2)$ is the joint distribution; $F(x_1)$ and $F(x_2)$ are the marginal distribution; u is equal to $F(x_1)$; v is equal to $F(x_2)$.

According to Sklar, the construction of joint distribution model requires two steps. Firstly, the marginal distribution needs to be constructed for each random variable; secondly, the copula function construction describing the correlation between variables needs to be determined. These two parts are independent steps, which is the advantage of copula theory over the traditional multivariate joint distribution construction method. The n-dimensional random vectors can be transformed into n one-dimensional marginal cumulative distribution functions and a copula function, derived from Eq.(1)

$$\begin{aligned} &f_{1,2,\cdots,n}(x_1,x_2,\cdots,x_n)\\ &=\prod_{i=1}^{n}\frac{\partial F_i(x_i)}{\partial x_i}\times\frac{\partial^n C_{1,2,\cdots,n}\left(F_1(x_1),F_2(x_2),\cdots,F_n(x_n)\right)}{\partial F_1(x_1)\partial F_2(x_2)\cdots\partial F_n(x_n)}\\ &=\prod_{i=1}^{n}f_i(x_i)\times D_{1,2,\cdots,n}\left(F_1(x_1),F_2(x_2),\cdots,F_n(x_n)\right)\\ &=D_{1,2,\cdots,n}(u_1,u_2,\cdots,u_n)\prod_{i=1}^{n}f_i(x_i) \end{aligned} \quad (2)$$

where $F_1(x_1)$, $F_2(x_2)$, $\cdots$, $F_n(x_n)$ are the one-dimensional marginal cumulative distribution functions; $C(u_1,u_2,\cdots u_n)$ is the copula function.

Through Eqs. (1) and (2), the multidimensional distribution model of uncertain parameters can be established. For the most common bivariate distribution model, the joint probability distribution can be expressed as follows

$$F(x_1,x_2)=C\left(F_1(x_1),F_2(x_2);\theta\right)=C(u_1,u_2;\theta) \quad (3)$$

$$f(x_1,x_2)=D(u_1,u_2;\theta)\,f_1(x_1)\,f_2(x_2) \tag{4}$$

where θ is the correlation parameter.

2.2 Analytical method of small sample test data

2.2.1 Mechanical parameters

Preliminary exploration tests and laboratory tests are not only of great significance for the assessment of potential geological disasters in geotechnical engineering and the stability of geotechnical structures but also provide guidance for estimating reliability risks and formulating risk plans. Rock mechanics parameters, including elastic modulus, Poisson's ratio, bulk density, shear strength and so on, can be obtained by sampling of geotechnical field and test in laboratory. Among them, elastic modulus, Poisson 's ratio, shear strength parameters (cohesion and internal friction angle) are the most common and basic test data in the geotechnical mechanical parameters. The statistical value of the geotechnical data often plays a significant role in the physical and mechanical properties. Existing experimental studies have shown that two shear strength parameters are statistically negatively correlated. (Baecher and Christian 2003), but the correlation of geotechnical mechanical parameters based on four mechanical parameters has not been studied. Therefore, a four-dimensional Gaussian copula joint probability distribution model with four mechanical parameters needs to be studied. Using Gaussian copula function to characterize the correlation characteristic of mechanical parameters has three advantages. Firstly, the Gaussian copula function can be uniquely confirmed by calculating the marginal distribution and correlation coefficient of uncertain parameter. Secondly, Compared with other copula functions, the correlation coefficient of Gaussian copula can be obtained [-1,1]. It can better describe the positive and negative correlation between variables. (3) After calculating and determining the correlation parameters between variables, the correlation parameter matrix can be obtained to construct the Gaussian copula function.

2.2.2 Four-dimensional Gaussian copula method

Based on Sklar's theorem, the first step is to calculate the optimal marginal functions for each parameter, and the second step is to establish the coupled model with multidimensional parameters. These two steps can be performed simultaneously. In the first step, the research on calculating the marginal distribution of each parameter has been relatively mature. Therefore, the key to the model of mechanical parameters lies in the construction of multi-dimensional copula model. This section first introduces the definition of multidimensional Gaussian copula, and then constructs the method of multidimensional Gaussian copula model. Thereafter, evaluates the fitting effect of three methods in the joint probability distribution of uncertain mechanical parameters.

(1) Function definition

$\Phi_\theta\left(\Phi^{-1}(u_1),\Phi^{-1}(u_2),\cdots,\Phi^{-1}(u_n);\theta\right)$ denotes the cumulative probability density with mean value of 0 and covariance matrix of θ. The covariance matrix is a semi-positive definite matrix with values of 1 on the diagonal. Then the cumulative probability density function of n-dimensional Gaussian copula is (Cherubini *et al.* 2004)

$$C_{1,2,\cdots,n}(u_1,u_2,\cdots,u_n;\theta)=\Phi_\theta\left(\Phi^{-1}(u_1),\Phi^{-1}(u_2),\cdots,\Phi^{-1}(u_n);\theta\right) \tag{5}$$

where $x_i=\Phi^{-1}(u_i)(i=1,2,\cdots,n)$. For multidimensional Gaussian copula, density function can be expressed as

$$\begin{aligned} D_{1,2,\cdots,n}(u_1,u_2,\cdots,u_n;\theta)&=\frac{\phi_{1,2,\cdots,n}(x_1,x_2,\cdots,x_n;\theta)}{\prod_{i=1}^{n}\phi(x_i)}\\ &=\frac{\frac{1}{(2\pi)^{n/2}\sqrt{|\theta|}}\exp\left(-\frac{1}{2}X^T\theta^{-1}X\right)}{\prod_{i=1}^{n}\frac{1}{\sqrt{2\pi}}\exp\left(-\frac{1}{2}x_i^2\right)}\\ &=|\theta|^{-\frac{1}{2}}\exp\left(-\frac{1}{2}X^T\left(\theta^{-1}-I\right)X\right) \end{aligned} \tag{6}$$

where $X=(x_1,x_2,\cdots,x_n)$ and $x_i=\Phi^{-1}(u_i)(i=1,2,\cdots,n)$. They are the multidimensional standard normal distribution variable obtained by the inverse function transformation of $(u_1,u_2,\cdots,u_n)$; I is the unit matrix.

(2) Modeling methods

Similar to the bivariate case, the correlation coefficient estimation methods of multidimensional Gaussian copula are Pearson method, Kendall method and Spearman method. Pearson correlation coefficient ρ can be expressed as

$$\rho=\frac{Cov(X_1,X_2)}{\sigma_1\sigma_2} \tag{7}$$

where $\mathrm{Cov}(X_1,X_2)$ represents the covariance of two variables, σ_1, σ_2 are the standard deviation of two variables.

For the Gaussian copula, the Eq. (7) can be simplified as follows

$$\rho=\frac{\exp(\zeta_1\zeta_2\theta)}{\sqrt{\exp(\zeta_1^2)-1}\sqrt{\exp(\zeta_2^2)-1}} \tag{8}$$

where ζ_1,ζ_2 represent the standard deviation when the marginal distribution of X_1, X_2 is lognormal distribution.

When the measured data are known, the Pearson coefficient ρ can be calculated by the equation below

$$\rho=\frac{\sum_{i=1}^{N}(x_{1i}-\bar{x}_1)(x_{2i}-\bar{x}_2)}{\sqrt{\sum_{i=1}^{N}(x_{1i}-\bar{x}_1)^2}\sqrt{\sum_{i=1}^{N}(x_{2i}-\bar{x}_2)^2}} \tag{9}$$

where $(x_{1i},i=1,2,\cdots,N)$,$(x_{2i},i=1,2,\cdots,N)$ represent a set of measured data of variables X_1, X_2 respectively; N is the samples; $\bar{x}_1$, $\bar{x}_2$ are the mean value of each group of samples respectively.

Compared with Pearson correlation coefficient, Kendall correlation coefficient depends on the order, so Kendall correlation coefficient remains unchanged when strictly monotonically increasing or decreasing transformation is performed. At the same time, Kendall correlation

coefficient τ and copula function parameter θ have the following relationship

$$\tau = 4\int_0^1\int_0^1 C(u_1,u_2;\theta)dC(u_1,u_2;\theta) - 1 \tag{10}$$

When the copula function is Gaussian copula, Eq. (10) can be expressed as

$$\theta = \sin\left(\frac{\pi}{2}\times\tau\right) \tag{11}$$

In engineering practice, when the measured data are known, τ can be obtained by the measured data X_1, X_2

$$\tau = \frac{\sum_{i<j} sign\left[\left(x_{1i}-x_{1j}\right)\left(x_{2i}-x_{2j}\right)\right]}{0.5N(N-1)} \tag{12}$$

where i, j=1,2,⋯, N; sign[·] denotes the sign function. N represents the total number in Eq. (11), the molecule represents the difference between the consistent and inconsistent combinations in the observation.

Spearman correlation coefficient represents the rank consistency between any independent identically distributed vector and sample population or distribution population.

The correlation of which is more similar to the population. At the same time, the relationship can be expressed as follows

$$\gamma = 12\int_0^1\int_0^1 C(u_1,u_2;\theta)du_1du_2 - 3 \tag{13}$$

When the copula function is Gaussian copula, Eq. (10) can be expressed as

$$\theta = 2\sin\left(\frac{\pi}{6}\times\gamma\right) \tag{14}$$

In engineering practice, when the measured data are known, Spearman correlation coefficient γ can be obtained from the equation below

$$\gamma=\rho\left(F_1(X_1),F_2(X_2)\right) \tag{15}$$

Combining Eqs. (9) and (15), the Spearman correlation coefficient can be obtained.

(3) Selection of the best copula

Select the suitable copula function to characterize the correlation of mechanical parameters is the key to reliability analysis of coal seam roof. In this section, the AIC criterion and the BIC criterion, which can better judge the fitting ability of copula function, are selected. The smaller AIC and BIC can be regarded as the most appropriate function.

The AIC criterion (Akaike 1974) is defined as the sum of the negative double of the logarithm of the probability density of the copula function. It can be expressed as follows

$$\mathrm{AIC} = -2\sum_{i=1}^{N}\ln D(u_{1i},u_{2i};\theta) + 2k \tag{16}$$

where k is the number of copula function. (u_{1i},u_{2i}) is as follows

$$\begin{cases} u_{1i} = \dfrac{\mathrm{rank}(x_{1i})}{N+1} \\ u_{2i} = \dfrac{\mathrm{rank}(x_{2i})}{N+1} \end{cases}, i = 1,2,\cdots,N \tag{17}$$

where rank(·) represents the ascending order.

The BIC criterion (Schwarz 1978) is defined as the sum of the negative double of the logarithm of the probability density value of the copula function at the original observation value of the variable and lnN times the number of copula function correlation parameters

$$\mathrm{BIC} = -2\sum_{i=1}^{N}\ln D(u_{1i},u_{2i};\theta) + k\ln N \tag{18}$$

3. Illustrative example

3.1 On-site exploration and test data samples

In this study, 176 sets of measured data of 31 coal mine roofs in China were collected. Each set of data contains the mechanical parameter information of geotechnical parameters, including elastic modulus, Poisson 's ratio, cohesion and internal friction angle. At the same time, the 176 sets of measured geotechnical data contain different soil properties, characteristics of coal mines and regions. The details are shown in Table 1. In Table 2, 176 sets of data from 31 coal mines are displayed in detail. In these data, the range of elastic modulus E is 0.16 ~ 82.4GPa, the range of Poisson 's ratio v is 0.08~0.44, the range of cohesion c is 0.17~25.6MPa, and the range of internal friction angle φ is 14~40.8°. Because it is difficult to express the correlation among multi-dimensional geotechnical parameters directly by Gaussian graph, in order to observe the correlation structure among geotechnical mechanical parameters intuitively, it is essential to express the correlation among each parameter by bivariate graph. Therefore, the four mechanical parameters selected in this section require six bivariate graphics to fully characterize the correlation. In Fig. 1(a)-1(f) are the measured distribution and empirical distribution of E and v, E and c, E and φ, v and c, v and φ, c and φ, respectively. u_1,u_2,u_3,u_4 represent the empirical distribution of E, v, c, φ, respectively.

According to the scatter distribution characteristics in the graph, the four parameters have different degrees of correlation. The measured points in (b) and (f) have certain correlation characteristics. Compared with the empirical distribution, the empirical distribution of E and c is mainly distributed near the 45° diagonal, which is basically symmetrical about the diagonal, and there is a strong positive correlation. The empirical distribution of c and φ is mainly distributed near the 135° diagonal, which is basically symmetrical about the diagonal with a strong negative correlation. The empirical distribution scatters in (a), (c), (d), (e) are relatively evenly dispersed and have no strong correlation. In addition, the empirical distribution between each two parameters is basically symmetrical about the diagonal, indicating that the measured geotechnical mechanical parameters (E,v,c,φ) have a basically symmetrical correlation structure. Based on the above 176 sets of measured data, four kinds of marginal distribution types are selected to test the AIC of each parameter by using Table 3, and the marginal distribution

Table 1 Sample test data

Number	Name of coal mine	Goaf roof conditions	Number of data sets
1	Xiadian gold deposits, north China (Zhu 2019)	inclined thick-large orebody	3
2	Xinpu phosphate deposit, Lianyungang City (Chen 2020)	hard rock mass	4
3	Yuanjiacun iron mine, Shanxi (Niu 2013)	Overburden goaf under open pit boundary	5
4	104 regiment coal mine, Xinjiang (He 2020)	steep coal seam mining area	13
5	Heilong coal mine, Shanxi (Guo 2019)	water-sprinkling roof	3
6	Qingdong coal mine, Anhui (Meng 2018)	hard roof	3
7	Cangshan iron mine, Shandong (Zhang 2010)	hard rock stratum roof	3
8	Zhujiaba copper mine, Yunnan (Dong 2020)	slightly inclined orebody	4
9	a coal mine in southwest China (Yang, 2018)	compound roof	6
10	Shennanwa coal mine, Shanxi (Zhao *et al.* 2021)	compound roof	12
11	a coal mine in Guizhou (Yu *et al.* 2020)	compound roof	4
12	Shilawusu coal mine, Inner Mongolia (Qiu 2016)	large section roadway roof	7
13	Xiaotun coal mine, Guizhou (Chen 2018)	compound roof	4
14	Panbei coal mine, Anhui (Chi 2021)	regenerative roof of large dip angle coal seam	9
15	Huangyuchuan coal mine, Inner Mongolia (Wu 2016)	layered roof	9
16	Huainan Panji mining area, Anhui (Shen 2020)	deep coal-bearing rock series	14
17	Linsheng coal mine, Liaoning (Chen *et al.* 2021)	hard roof of steeply inclined coal seam	4
18	Jingcheng coal mine, Shanxi (Wu 2022)	water-drenched surrounding rock roof	3
19	Heilong coal mine, Shanxi (Guo *et al.* 2019)	water-sprinkling roof	3
20	Datunsong mine, Yunnan (Shang 2018)	complex orebody of large goaf	3
21	Zhaozhuang mine, Shanxi (Zhao 2020)	compound roof	6
22	Dongdong coal mine, Shaanxi (Liu 2018)	compound roof	6
23	Zhujixi coal mine, Anhui (Meng *et al.* 2017)	compound roof	3
24	Shenzhou coal mine, Shanxi (Su 2013)	extra-thick compound roof	6
25	Hengsheng coal mine, Shanxi (Li 2012)	hard roof	2
26	Zhaozhuang mine, Shanxi (Li 2017)	layered roof	4
27	East Kouzi coal mine, Anhui (Shen 2015)	component roof	6
28	Baode coal mine, Shanxi (Dou 2021)	thick coal-seam with hard roof	13
29	Shuangxin coal mine, InnerMongolia (Jiao 2021)	soft roof	3
30	Sanjiaohe coal mine, Shanxi (Sun 2015)	roof near fault	7
31	Ann hill coal mine, Shaanxi (Peng 2012)	layered roof	4

AIC calculation results of each group of parameters are shown in Table 4. As can be seen from Table 4, in the statistical measured data, the marginal distribution type of elastic modulus and cohesion are logarithmic normal distribution, and the marginal distribution type of Poisson 's ratio and cohesion are normal distribution. The calculation results of Table 4 and the statistical values of the measured data are sorted out. The results are shown in Table 5.

It can be analyzed from Table 5 that the coefficient of variation of the four parameters is bulky. Among them, the coefficient of variation of parameters X_1 and X_3 is above 1, which reflects that the collected measured geotechnical data have a wide range of sources, and the properties of coal mine are quite different. The reasons for the large dispersion of these data may be due to: (1) the number of samples obtained by the survey test is little, and it is often more arduous to obtain general patterns based on limited test data, which makes the data results greatly variable. (2) There are considerable types of roofs collected, and the distribution of sources is uneven. Combined with Table 1, it shows that most of the roof types are composite roofs, and there are extensive types of rock strata. (3) Due to the errors in the test process such as sample transportation and laboratory tests. After constructing the marginal distribution model of mechanical parameters, the multidimensional Gaussian copula function is used to characterize the correlation structure between the four parameters. Table 6 shows three correlation coefficient matrices calculated using Pearson, Kendall, and Spearman methods respectively.

It can be observed that the correlation between the geotechnical mechanical parameters is different. For example, there is a strong positive correlation between elastic modulus E and cohesion c; there is a strong negative correlation between shear strength parameters c and φ, which is also consistent with a large number of statistical studies. There exists a positive correlation between Poisson 's ratio ν and cohesion c, but the correlation is weak. The negative correlation between the modulus of elasticity E and the angle of internal friction φ is weaker than the negative correlation between the shear strength parameters. Similarly, Poisson's ratio v is weakly positively correlated with the internal friction angle φ, which is basically consistent with the conclusion obtained in Fig. 1. However, due to the different construction methods, the correlation coefficient between elastic modulus E and

Table 2 The specific value of mechanical parameters

Number	*E*(GPa)	*v*	*c*(MPa)	*φ*(°)	Number	*E*(GPa)	*v*	*c*(MPa)	*φ*(°)
1#	1.35	0.34	1.65	34	15#	8.72	0.42	5	33
1#	1.26	0.32	1.46	35	16#	42.6	0.35	4.54	29.68
1#	1.56	0.33	1.78	37	16#	27.6	0.13	3.13	30.88
2#	6.23	0.27	8.21	34.35	16#	34.38	0.18	3.77	30.68
2#	3.51	0.18	5.56	32	16#	15	0.1	1.27	34.64
2#	5.01	0.22	6.89	30	16#	28.68	0.18	6.52	30.33
2#	3.7	0.21	4.6	30	16#	12.66	0.08	1.36	34.23
3#	14.23	0.142	0.71	39.11	16#	36.09	0.16	5.84	30.92
3#	9.97	0.203	0.67	39.89	16#	60	0.4	11	25
3#	11.97	0.211	1.05	34.97	16#	4.24	0.08	1.09	37.86
3#	8.98	0.171	0.52	36.8	16#	23.2	0.2	4.3	31.78
3#	12.83	0.121	0.47	40.15	16#	36	0.4	16	20
4#	1.6	0.17	2.6	31.6	16#	15.73	0.22	2.87	32.98
4#	0.16	0.27	1.33	31.8	16#	7.58	0.12	0.61	30.48
4#	1.6	0.17	2.98	30.8	16#	22.16	0.21	2.71	34.52
4#	0.15	0.21	1.28	33	17#	8.511	0.19	2.9	36
4#	1.76	0.17	3	40.5	17#	2.96	0.2	2.9	37
4#	0.16	0.2	1.55	34	17#	5.811	0.2	11.5	33
4#	1.6	0.17	2.58	29.2	17#	5.364	0.24	6.4	25
4#	0.17	0.2	1.5	36.2	18#	12.1	0.28	9.41	31.6
4#	1.6	0.17	2.4	40.8	18#	7.95	0.17	0.17	36.7
4#	0.16	0.24	1.59	35	18#	6.2	0.22	0.22	36.6
4#	1.6	0.17	2.58	38.8	19#	11	0.26	9.38	30.65
4#	0.16	0.2	1.54	36	19#	8.23	0.18	5.44	23.77
4#	1.1	0.21	2.3	37.5	19#	6.15	0.21	4.13	20.84
5#	11	0.26	9.38	30.65	20#	3.6	0.114	0.185	38.11
5#	8.23	0.18	5.44	23.77	20#	9.08	0.248	0.322	37.69
5#	6.15	0.21	4.13	30.84	20#	7.58	0.161	0.286	32.71
6#	12.55	0.18	4.41	29.57	21#	14.72	0.39	2.25	32
6#	22.35	0.16	5.25	28.86	21#	36.43	0.28	4.63	26
6#	3.49	0.22	0.52	32.9	21#	58.56	0.24	12.09	28
7#	37.16	0.22	13.66	31.5	21#	25.6	0.23	18.41	26
7#	37.49	0.21	12.64	31.6	21#	74.35	0.22	21.75	23
7#	44.23	0.18	13.93	28	21#	19.21	0.18	15.36	17
8#	8.34	0.24	0.512	37.1	22#	19.5	0.2	2.75	28
8#	6.69	0.33	0.41	38.02	22#	8.75	0.26	1.2	36
8#	12.87	0.29	0.84	36.22	22#	0.99	0.31	1	35
8#	18.42	0.25	0.59	36.88	22#	1.5	0.33	2.6	39
9#	0.445	0.33	2	35	22#	5.8	0.28	4.9	25.2
9#	1.938	0.32	2.5	28	22#	5.99	0.2	4	37
9#	0.445	0.33	2	35	23#	70.5	0.21	9.52	29.51
9#	1.635	0.32	2.5	28	23#	59.7	0.25	5.67	30.36
9#	0.445	0.33	2	35	23#	4.52	0.26	0.6	35
9#	0.926	0.32	2.5	28	24#	2.898	0.24	2.49	21.06
10#	27.69	0.29	6.86	34.17	24#	6.965	0.25	6.02	25.82
10#	34.63	0.18	11.61	34.32	24#	4.967	0.22	8.38	22.73
10#	29.56	0.32	7.65	37.21	24#	2.684	0.31	3.7	23.77
10#	39.79	0.37	12.04	31.22	24#	4.729	0.24	2.85	26.62
10#	3.49	0.38	0.85	35.88	24#	1.395	0.24	7.03	27.52
10#	22.59	0.23	5.74	37.09	25#	16.028	0.11	15.74	20
10#	34.6	0.18	17.03	22.42	25#	50.226	0.34	18.46	18.5
10#	22.59	0.23	5.74	37.09	26#	74.35	0.22	21.75	18
10#	3.49	0.38	0.85	35.88	26#	58.56	0.24	12.09	28
10#	22.59	0.28	12.04	26.3	26#	36.43	0.28	4.63	26
10#	34.6	0.18	22.56	21.5	26#	14.72	0.39	2.25	22
10#	34.6	0.12	10.38	30.7	27#	4.6	0.25	2	25
11#	4.038	0.28	24.3	23	27#	11.62	0.3	5	35
11#	1.938	0.32	10.8	30	27#	4	0.2	1.4	23
11#	1.635	0.32	10.8	25	27#	3.1	0.2	0.8	20
11#	0.926	0.32	10.8	25	27#	9.83	0.3	3.5	32
12#	10.85	0.147	2.5	27	27#	5.6	0.25	2.5	29
12#	33.4	0.235	3.2	30	28#	6.03	0.22	1.18	35
12#	5.425	0.147	2.5	27	28#	2.43	0.31	0.5	34
12#	19.5	0.2	3.1	32	28#	6.03	0.22	1.18	35
12#	17.7	0.204	2	30	28#	6.03	0.22	1.18	35
12#	5.425	0.147	2.5	27	28#	10.45	0.3	0.7	36
12#	5.425	0.147	2.5	27	28#	16.9	0.22	1.18	35
13#	4.038	0.28	5.3	33	28#	20.8	0.17	3.8	33
13#	1.938	0.32	2.5	30	28#	6.03	0.22	1.18	35
13#	3.835	0.29	2.5	30	28#	2.43	0.31	0.5	36
13#	1.926	0.32	2.5	30	28#	10.45	0.3	0.7	36
14#	9.5	0.28	1.2	30	28#	2.43	0.31	0.5	36
14#	18	0.18	2.6	28	28#	10.45	0.3	0.7	36
14#	9.5	0.28	1.2	30	28#	15.15	0.17	0.7	36
14#	15	0.2	2.4	35	29#	6.28	0.24	3.16	25.6
14#	18	0.18	2.6	28	29#	4.71	0.32	2.43	35.3
14#	9.5	0.28	1.2	30	29#	2.15	0.21	2.21	24.3
14#	9.5	0.28	1.2	30	30#	10.6	0.3	3.2	32
14#	18	0.18	2.6	38	30#	8.2	0.23	3.2	27
14#	9.5	0.28	1.2	30	30#	82.4	0.3	26	16
15#	25.5	0.21	13.1	14	30#	48.1	0.2	11.5	27
15#	22.8	0.19	5.9	30	30#	7.1	0.32	5	30
15#	23.6	0.17	11.8	15	30#	7.2	0.23	3.2	25
15#	21.7	0.17	9.6	26	30#	8.2	0.23	3.2	31
15#	36.3	0.44	9.6	23	31#	25.2	0.27	15.5	20
15#	5.19	0.24	4.1	34	31#	26.2	0.29	17.5	22
15#	45.7	0.3	4.9	35	31#	17.5	0.26	25.6	17
15#	11.6	0.43	8.4	35	31#	5.2	0.39	4.6	28
		measured data					empirical distribution		

Poisson 's ratio *v* has both positive and negative values, indicating that there is a certain uncertainty in the characterization of the correlation of different construction methods. Therefore, to further study the correlation structure between the four-dimensional mechanical parameters and the multi-dimensional joint distribution

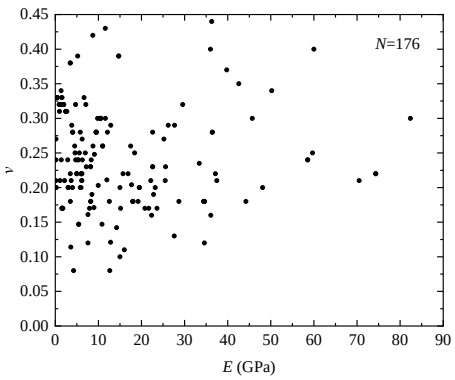

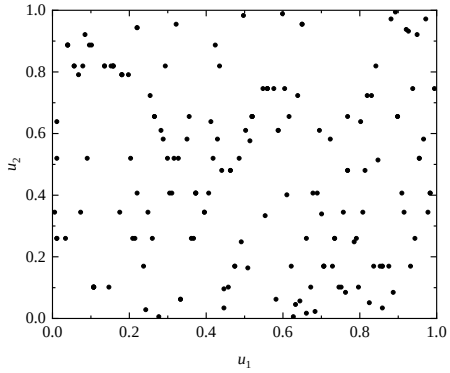

(a) E and v

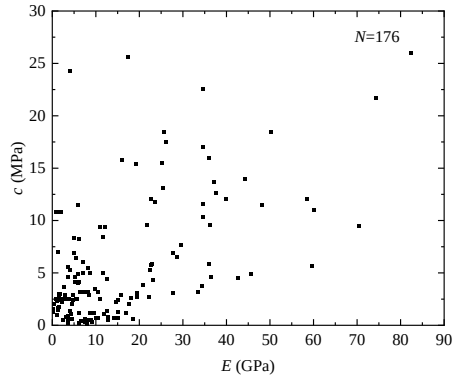

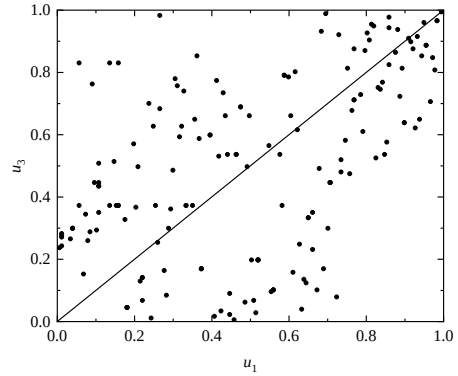

(b) E and c

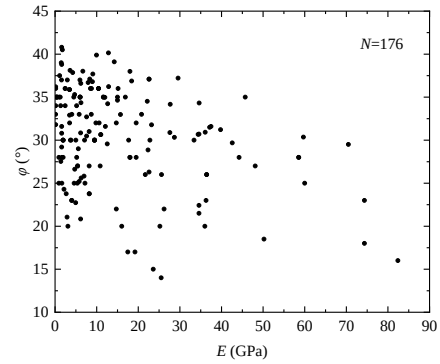

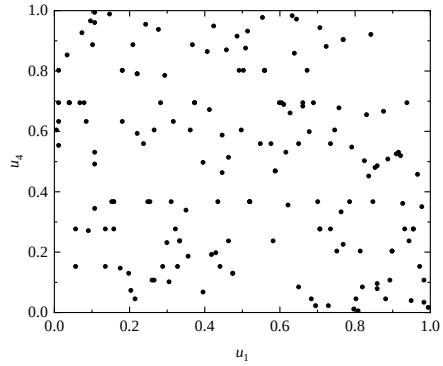

(c) E and φ

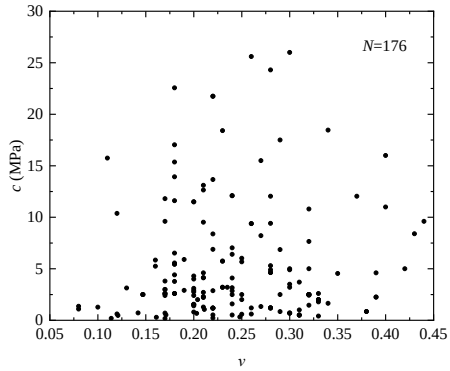

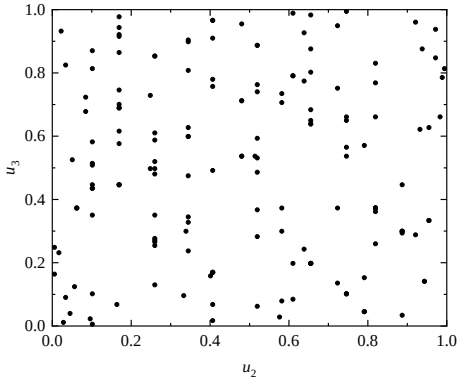

(d) v and c

Fig. 1 Measured mechanical parameters and empirical distribution

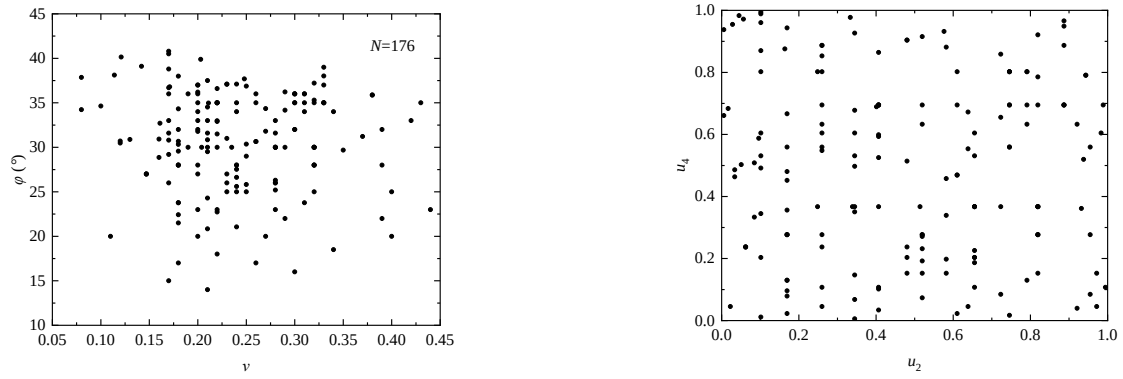

(e) v and φ

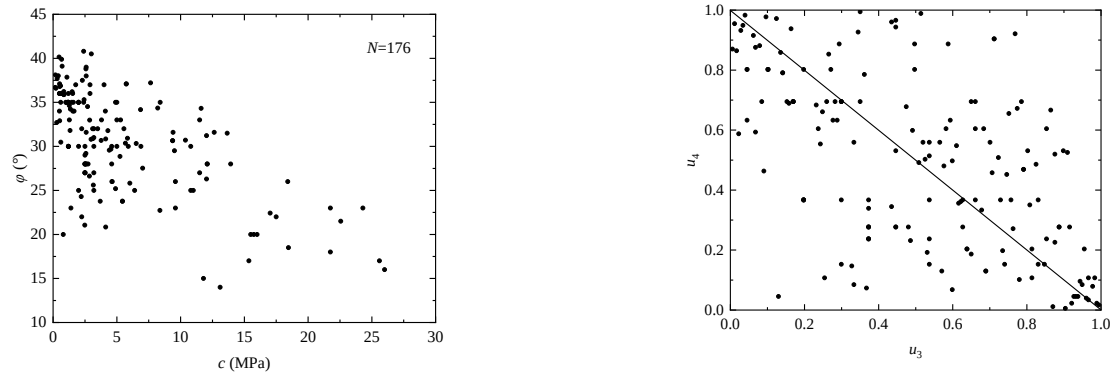

(f) c and φ

Fig. 1 Continued-

Table 3 Statistical distribution functions

distribution type	$F(x)$	$f(x)$	mean value μ, variance σ^2
Normal	$\Phi\left(\frac{x-p}{q}\right)$	$\frac{1}{q\sqrt{2\pi}}\times\exp\left[-\frac{(x-p)^2}{2q^2}\right]$	$\mu=p$ $\sigma^2=q^2$
Lognormal	$\Phi\left(\frac{\ln x-p}{q}\right)$	$\frac{1}{q\sqrt{2\pi}}\times\exp\left[-\frac{(\ln x-p)^2}{2q^2}\right]$	$\mu=\exp\left(p+0.5q^2\right)$ $\sigma^2=\left[\exp\left(q^2\right)-1\right]$ $\times\exp\left(2p+q^2\right)$
Extreme value type I	$1-\exp\left\{-\exp\left[-(x-p)/q\right]\right\}$	$(1/q)\exp\left[(x-p)/q\right]$ $\times\exp\left[-\exp(x-p)/q\right]$	$\mu=p+0.5772q$ $\sigma^2=\pi^2q^2/6$
Gamma	$\frac{1}{\Gamma(p)}\Upsilon\left(p,\frac{x}{q}\right)$	$\frac{1}{\Gamma(p)q^p}x^{p-1}e^{-x/q}$	$\mu=pq$ $\sigma^2=pq^2$

Note: $\Phi(\cdot)$ is the standard normal distribution function; $\Upsilon(\cdot)$ is a low order incomplete gamma function; $\Gamma(\cdot)$ is a gamma function

model are of great significance. By calculating the correlation coefficient matrix obtained by the three construction methods, the Gaussian copula model can be constructed by using the Eqs. (8), (11) and (14). The AIC and BIC criteria are used to calculate the fitting effect of the copula model. The correlation parameter matrix and AIC and BIC values of the Gaussian copula under the three construction methods are calculated as shown in Table 7 below. When using the Pearson method to calculate the correlation parameters, due to the solution and iteration of the double integral, in order to reduce the calculation cost, the marginal distribution of the parameters X_2 and X_4 is regarded as the lognormal distribution consistent with X_1 and X_3, and the Eq. (14) is used to calculate the correlation parameters.

Table 7 shows that the AIC and BIC of the correlation parameter matrix calculated by the Pearson method are 419.2 and 438.22; the fitting effects of the two rank correlation methods are similar. The AIC and BIC values of the Kendall method are 74.84 and 93.86 respectively, which

Table 4 AIC value of different marginal distribution

distribution type	$X_1=E$	$X_2=v$	$X_3=c$	$X_4=\varphi$
Normal	1487.6	**-260.5**	1105	**1113.8**
Lognormal	**-476.2**	40850	**-422**	4261.1
Extreme value type I	1845.9	—	1423.5	1140.2
Gamma	13824	652.3	3062.6	10993

Table 5 Geomechanical parameters distribution and statistical characteristics

parameters	mean value	variance	coefficient of variation COV	distribution type
$X_1=E$(Gpa)	14.926	268.232	1.097	Lognormal
$X_2=v$	0.248	0.013	0.46	Normal
$X_3=c$(MPa)	5.236	30.509	1.055	Lognormal
$X_4=\varphi$(°)	30.569	32.069	0.185	Normal

Table 6 Correlation coefficient matrices

correlation parameters	correlation coefficient matrix
Pearson correlation parameters ρ	$\begin{bmatrix} 1 & 0.063 & 0.618 & -0.359 \\ 0.063 & 1 & 0.082 & -0.096 \\ 0.618 & 0.082 & 1 & -0.632 \\ -0.359 & -0.096 & -0.632 & 1 \end{bmatrix}$
Kendall correlation parameters τ	$\begin{bmatrix} 1 & -0.087 & 0.342 & -0.173 \\ -0.087 & 1 & 0.028 & -0.020 \\ 0.342 & 0.028 & 1 & -0.425 \\ -0.173 & -0.020 & -0.425 & 1 \end{bmatrix}$
Spearman correlation parameters γ	$\begin{bmatrix} 1 & -0.119 & 0.434 & -0.255 \\ -0.119 & 1 & 0.050 & -0.022 \\ 0.434 & 0.050 & 1 & -0.573 \\ -0.255 & -0.022 & -0.573 & 1 \end{bmatrix}$

Table 7 Four-dimensional Gaussian Copula model and goodness of fit

constructive method	correlation coefficient matrix	AIC	BIC
Pearson method	$\begin{bmatrix} 1 & 0.081 & 0.702 & -0.465 \\ 0.081 & 1 & 0.103 & -0.103 \\ 0.702 & 0.103 & 1 & -0.83 \\ -0.465 & -0.103 & -0.83 & 1 \end{bmatrix}$	419.2	438.22
Kendall method	$\begin{bmatrix} 1 & -0.136 & 0.512 & -0.268 \\ -0.136 & 1 & 0.044 & -0.031 \\ 0.512 & 0.044 & 1 & -0.619 \\ -0.268 & -0.031 & -0.619 & 1 \end{bmatrix}$	**74.84**	**93.86**
Spearman method	$\begin{bmatrix} 1 & -0.124 & 0.45 & -0.266 \\ -0.124 & 1 & 0.052 & -0.021 \\ 0.45 & 0.052 & 1 & -0.591 \\ -0.266 & -0.021 & -0.591 & 1 \end{bmatrix}$	83.39	102.41

is the optimal construction method. The AIC and BIC values of the Spearman method are 83.36 and 102.41 respectively. The two rank correlation coefficient construction methods are significantly superior than the Pearson method. The reason for the difference between the applicability evaluation conclusion of the construction method of the common copula model and other copula models is that when the Pearson linear correlation

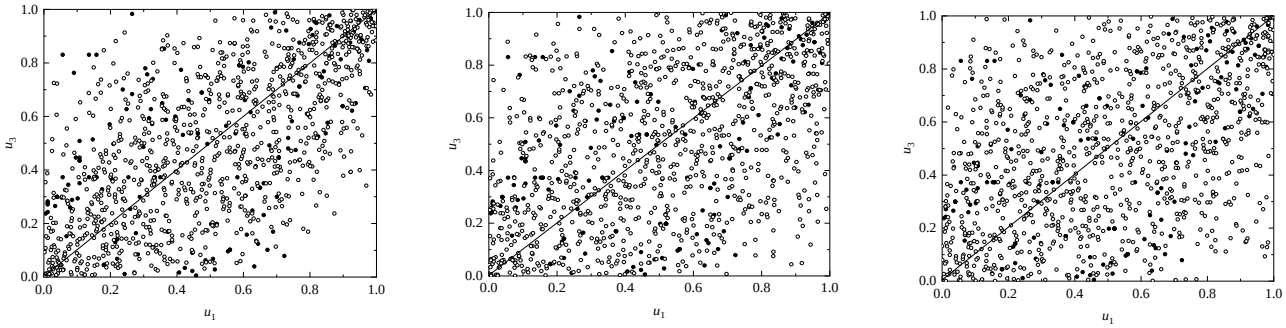

Fig. 2 Empirical distribution of measured parameters (E,c) and scatter diagram of simulated variable U. (a) Pearson method, (b) Kendall method and (c) Spearman method

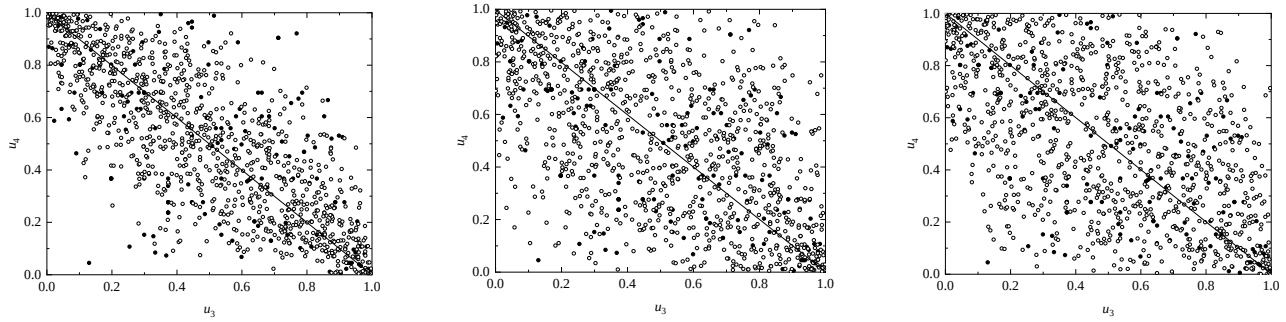

Fig. 3 Empirical distribution of measured parameters (c,φ) and scatter diagram of simulated variable U. (a) Pearson method, (b) Kendall method and (c) Spearman method

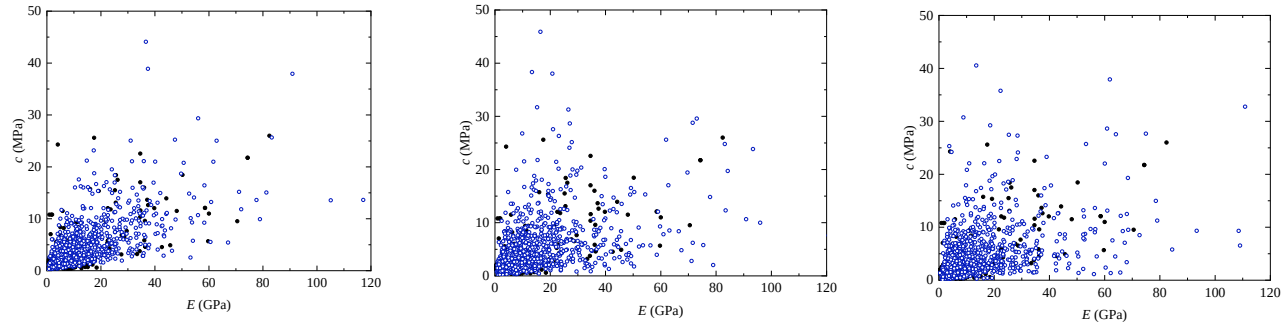

Fig. 4 Original distribution of measured parameters (E,c) and simulated variable X. (a) Pearson method, (b) Kendall method and (c) Spearman method

coefficient is used to construct the Gaussian copula, the correlation parameters obtained are not only related to thecorrelation coefficient matrix, but also related to the parameter marginal distribution function. When the copula model is constructed by the Pearson method, the parameter X_2 and X_4 marginal parameter distribution is also approximately regarded as the lognormal distribution, so the model constructed by the Pearson method has a large error.

In addition, the error of the Pearson method is further enlarged due to the fact that the Pearson method solves for the correlation parameter without an explicit analytical expression, and can only be solved by a complicated double integration.

3.2 Multidimensional joint distribution

After establishing the distribution model of mechanical parameters, this section will simulate the multidimensional joint distribution model based on the model. First, the probability value of each parameter under the standard uniform distribution is generated, that is, $U_i=F_i(X_i)$; Then the simulated variable $U_i=F_i(X_i)$ is mapped to the original space according to the principle of equal probability transformation to obtain the simulated sample $X_i=F_i(U_i)$ which obeys the four-dimensional Gaussian copula. Since the bivariate graphs convey similar information effects, two sets of parameters with strong positive correlation (E,c) and strong negative correlation (c,φ) are selected in this section to compare the fitting effects of the four-dimensional Gaussian copula model under disparate construction methods. The Monte-Carlo method is used to simulate 1000 samples. Figs. 2 and 3 show the scatter plots of the standard uniform distribution variable U under the three construction methods. The black solid dots represent the empirical distribution points of the measured data, and the black hollow dots represent the simulated sample points.

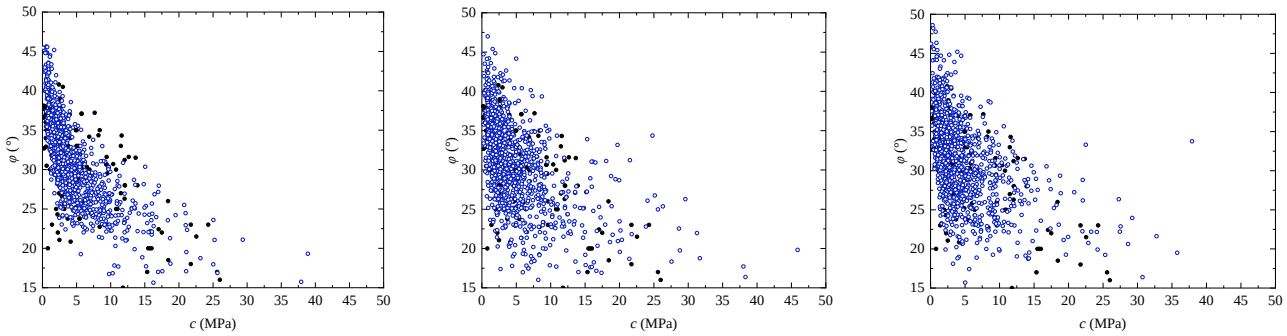

Fig. 5 Original distribution of measured parameters (c, φ) and simulated variable X. (a) Pearson method, (b) Kendall method and (c) Spearman method

Table 8 Simulation error of Pearson correlation coefficient under different construction methods

constructive method	ρ_U Calculated by Simulated Variable U	ρ_X Calculated by Simulated Variable X	$\lvert\rho_X-\rho\rvert$
Pearson method	$\begin{bmatrix} 1 & 0.083 & 0.671 & -0.425 \\ 0.083 & 1 & 0.138 & -0.147 \\ 0.671 & 0.138 & 1 & -0.817 \\ -0.425 & -0.147 & -0.817 & 1 \end{bmatrix}$	$\begin{bmatrix} 1 & 0.090 & 0.615 & -0.390 \\ 0.090 & 1 & 0.127 & -0.157 \\ 0.615 & 0.127 & 1 & -0.701 \\ -0.390 & -0.157 & -0.701 & 1 \end{bmatrix}$	**[0.003, 0.069]**
Kendall method	$\begin{bmatrix} 1 & 0.057 & 0.482 & -0.290 \\ 0.057 & 1 & 0.093 & -0.099 \\ 0.482 & 0.093 & 1 & -0.620 \\ -0.290 & -0.099 & -0.620 & 1 \end{bmatrix}$	$\begin{bmatrix} 1 & 0.057 & 0.482 & -0.289 \\ 0.057 & 1 & 0.093 & -0.099 \\ 0.482 & 0.093 & 1 & -0.620 \\ -0.289 & -0.099 & -0.620 & 1 \end{bmatrix}$	**[0.004, 0.136]**
Spearman method	$\begin{bmatrix} 1 & 0.073 & 0.625 & -0.360 \\ 0.073 & 1 & 0.109 & -0.107 \\ 0.625 & 0.109 & 1 & -0.751 \\ -0.360 & -0.107 & -0.751 & 1 \end{bmatrix}$	$\begin{bmatrix} 1 & 0.065 & 0.593 & -0.355 \\ 0.090 & 1 & 0.144 & -0.147 \\ 0.593 & 0.144 & 1 & -0.802 \\ -0.355 & -0.147 & -0.802 & 1 \end{bmatrix}$	**[0.002, 0.170]**

Table 9 Simulation error of Kendall correlation coefficient under different construction methods

constructive method	τ_U Calculated by Simulated Variable U	τ_X Calculated by Simulated Variable X	$\lvert\rho_X-\rho\rvert$
Pearson method	$\begin{bmatrix} 1 & -0.128 & 0.494 & -0.213 \\ -0.128 & 1 & 0.050 & -0.038 \\ 0.494 & 0.050 & 1 & -0.583 \\ -0.213 & -0.038 & -0.583 & 1 \end{bmatrix}$	$\begin{bmatrix} 1 & -0.128 & 0.494 & -0.213 \\ -0.128 & 1 & 0.050 & -0.038 \\ 0.494 & 0.050 & 1 & -0.583 \\ -0.213 & -0.038 & -0.583 & 1 \end{bmatrix}$	**[0.018, 0.158]**
Kendall method	$\begin{bmatrix} 1 & -0.084 & 0.341 & -0.144 \\ -0.084 & 1 & 0.035 & -0.025 \\ 0.341 & 0.035 & 1 & -0.409 \\ -0.144 & -0.025 & -0.409 & 1 \end{bmatrix}$	$\begin{bmatrix} 1 & -0.084 & 0.341 & -0.144 \\ -0.128 & 1 & 0.035 & -0.025 \\ 0.341 & 0.035 & 1 & -0.409 \\ -0.144 & -0.025 & -0.409 & 1 \end{bmatrix}$	**[0.001, 0.029]**
Spearman method	$\begin{bmatrix} 1 & -0.109 & 0.340 & -0.193 \\ -0.109 & 1 & 0.061 & -0.033 \\ 0.460 & 0.061 & 1 & -0.498 \\ -0.193 & -0.033 & -0.498 & 1 \end{bmatrix}$	$\begin{bmatrix} 1 & -0.109 & 0.340 & -0.193 \\ -0.109 & 1 & 0.061 & -0.033 \\ 0.460 & 0.061 & 1 & -0.498 \\ -0.193 & -0.033 & -0.498 & 1 \end{bmatrix}$	**[0.002, 0.073]**

In the simulation data of the parameter group (E, c) with obvious positive correlation and the parameter group (c, φ) with negative correlation. The sample points simulated by Pearson method are concentrated in the diagonal area, and there are still many measured solid points scattered outside the simulation area. The areas covered by the black hollow simulation points simulated by the two rank correlation coefficient methods are significantly larger than that of the measured solid points, which have better fitting ability.

Figs. 4 and 5 show the scatter plots of the relevant standard uniform distribution variable X under the three construction methods. The black solid dots represent the measured data points, and the blue hollow dots represent the simulated sample points in the original space after equal probability transformation. From the information obtained from Figs. 4 and 5, it can be observed that the distribution of the simulated sample points constructed by the three methods is mainly concentrated in the dense area of the

Table 10 Simulation error of Spearman correlation coefficient under different construction methods

constructive method	γ_U Calculated by Simulated Variable U	γ_X Calculated by Simulated Variable X	$\lvert\rho_X - \rho\rvert$
Pearson method	$\begin{bmatrix} 1 & -0.084 & 0.302 & -0.147 \\ -0.084 & 1 & 0.072 & -0.030 \\ 0.302 & 0.072 & 1 & -0.475 \\ -0.147 & -0.030 & -0.475 & 1 \end{bmatrix}$	$\begin{bmatrix} 1 & -0.084 & 0.302 & -0.147 \\ -0.084 & 1 & 0.072 & -0.030 \\ 0.302 & 0.072 & 1 & -0.475 \\ -0.147 & -0.030 & -0.475 & 1 \end{bmatrix}$	**[0.008, 0.132]**
Kendall method	$\begin{bmatrix} 1 & -0.125 & 0.395 & -0.217 \\ -0.125 & 1 & 0.106 & -0.045 \\ 0.395 & 0.106 & 1 & -0.539 \\ -0.217 & -0.045 & -0.539 & 1 \end{bmatrix}$	$\begin{bmatrix} 1 & -0.125 & 0.395 & -0.217 \\ -0.125 & 1 & 0.106 & -0.045 \\ 0.395 & 0.106 & 1 & -0.539 \\ -0.217 & -0.045 & -0.539 & 1 \end{bmatrix}$	**[0.006, 0.056]**
Spearman method	$\begin{bmatrix} 1 & -0.105 & 0.440 & -0.270 \\ -0.105 & 1 & 0.050 & -0.039 \\ 0.440 & 0.050 & 1 & -0.562 \\ -0.270 & -0.039 & -0.562 & 1 \end{bmatrix}$	$\begin{bmatrix} 1 & -0.105 & 0.440 & -0.270 \\ -0.105 & 1 & 0.050 & -0.039 \\ 0.440 & 0.050 & 1 & -0.562 \\ -0.120 & -0.039 & -0.562 & 1 \end{bmatrix}$	**[0.000, 0.017]**

Table 11 The correlation parameter θ calculated by different Copula functions

parameter	Gaussian	Plackett	Frank	Clayton	No.16
(E, c)	0.512	8.863	3.290	1.040	—
(c, φ)	-0.619	0.142	-4.516	—	0.022

measured points, especially near the mean value of the parameters. However, there are still a certain number of black measured points falling outside the simulation area in the results obtained by the Pearson method. Compared with the Pearson method, the sample X distribution simulated by the two rank correlation coefficient methods is more accurate, reflecting the superiority of the rank correlation coefficient method. After obtaining the Gaussian copula simulation sample U and its distribution sample X in the original space, Tables 8-10 show the Pearson, Kendall and Spearman of the simulation sample U and the partial sample X of the original space under each construction method, then calculate the simulation error of each method.

Table 8 shows that there is still a certain gap between the Pearson correlation coefficient of the simulated sample and original observation data. The gap between the simulated variable U and the simulated variable X is also gargantuan. This is because when the simulated variable U is transformed into the original space with equal probability, its parameter marginal distribution also changes. From the difference between the simulated variable X and the measured data, it appears that the Pearson correlation coefficient obtained by the Pearson method under the three construction methods is the best, and the simulation error is an order of magnitude smaller than the other two rank correlation methods. The simulation effect of the two rank correlation methods is similar, and the Spearman method is slightly better than the Kendall method. From Tables 9 and 10, it is evident that the Kendall and Spearman calculated by the three construction methods under uniform distribution are the same as those calculated in the original space. This is owing to the rank of the samples is consistent in both the uniform distribution space and the original space when the rank correlation coefficient is calculated. For the Kendall correlation coefficient τ, the simulation error of the Kendall method is the smallest among the three construction methods. The second is the Spearman method, the order of magnitude of the error is consistent with the Kendall method. The Pearson method with the largest error is one order of magnitude larger than the rank correlation method. For the Spearman rank correlation coefficient γ, the construction method with the smallest simulation error is the Spearman method. The second is the Kendall method, whose error order of magnitude is consistent with the Spearman method. The largest simulation error is the Pearson method, whose simulation error is an order of magnitude larger than the rank correlation method. Therefore, considering the three correlation coefficients, the simulation error is the smallest when the construction method consistent with the correlation coefficient is used. The simulation errors of the two rank correlation methods are relatively close, and the error range of the Pearson method is larger when simulating different correlation coefficients.

3.3 Influence of different copula functions

3.3.1 Correlation characteristic

In order to quantitatively compare the influence of copula functions on the positive and negative correlation between parameters, Gaussian copula, Plackett copula, Frank copula, Clayton copula and No.16 copula are selected as alternative copula to test the influence on the correlation structure between parameters. Table 11 calculates the correlation parameter values of the two sets of parameters under different copula functions, then uses the AIC criterion to calculate the AIC values of the two sets of parameters. Date in Table 12 suggest that the Gaussian copula function in the positive and negative two sets of parameters is the optimal copula function identified. The AIC value of the

Table 12 AIC values calculated by different Copula functions

parameter	Gaussian	Plackett	Frank	Clayton	No.16
(E, c)	**-46.043**	-14.851	-43.353	23.445	—
(c, φ)	**-76.789**	-71.699	-69.738	—	-18.602

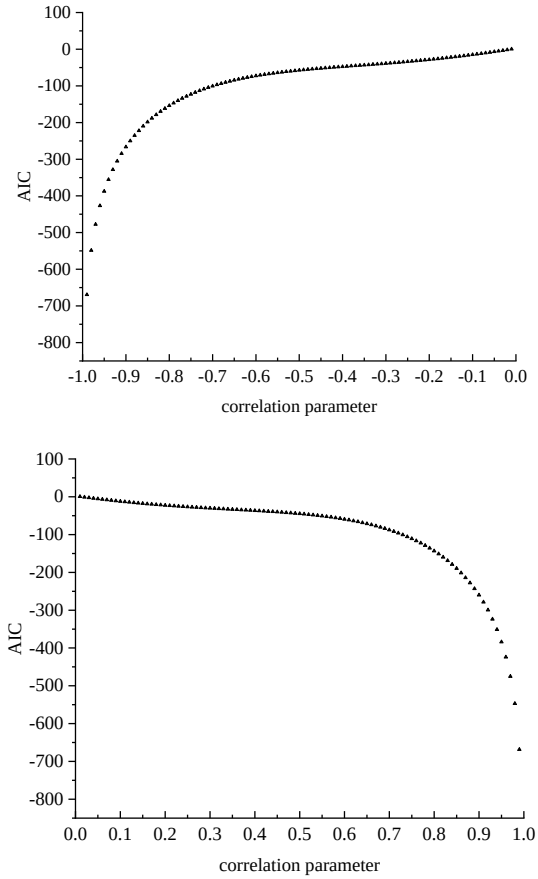

Fig. 6 Gaussian copula fitting ability. (a) negative correlation variation curve and (b) positive correlation variation curve

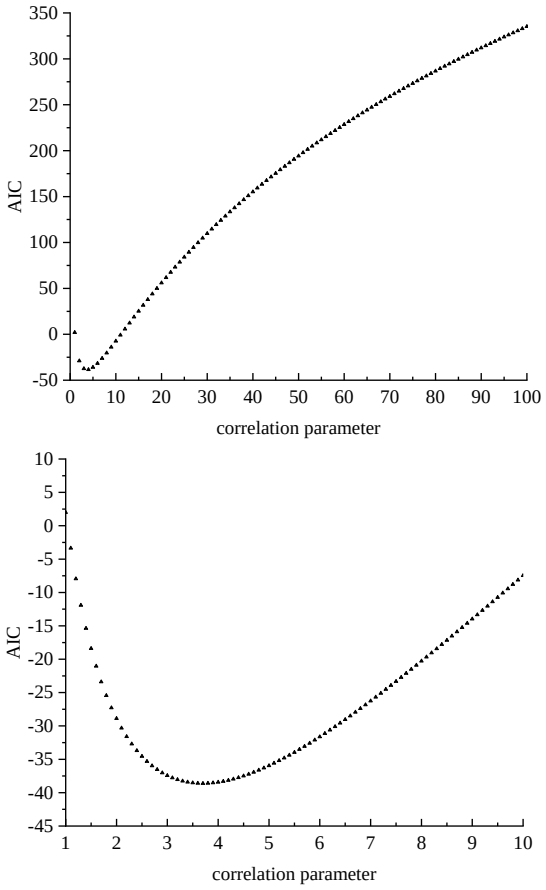

Fig. 7 Plackett copula fitting ability curve with positive correlation. (a) θ from 0 to 100 and (b) θ from 1 to 10

Frank copula function between (E,c) parameters is slightly larger than that of the Gaussian copula. The AIC values calculated by Plackett copula and Frank copula between (c,φ) parameters are clearly close to the AIC values calculated by Gaussian copula. As a copula function which can describe the positive and negative correlation between parameters, Gaussian copula still has good universality and stability. Therefore, in engineering practice, when selecting copula function for positive correlation parameters and negative correlation parameters, it is indispensable to carry out actual calculation to determine the final copula function, and Gaussian copula cannot be simply selected as the optimal copula.

3.3.2 Fitting ability

In view of the value range of the relevant parameters of different copula functions is diverse, in order to consider the fitting effect of different copula functions with strong correlation and weak correlation, this section calculates the AIC value of the correlation parameters of the selected bivariate copula function under the condition of modeling measured data. The calculation results are shown from Figs. 6 to 12. As detailed in these figures, the fitting ability of disparate copula functions varies significantly with the change of correlation. In Fig. 6, the fitting ability of Gaussian copula increases exponentially with the increase of correlation when the parameters are positively or negatively correlated. The deformation curve of the fitting ability of the parameters with positive correlation and negative correlation shows obvious symmetry about θ=0. As can be seen in Fig. 7, the Plackett copula positive correlation fitting ability curve increases first and then decreases with the increase of positive correlation. Besides, the fitting ability reaches the peak when θ is between 3 and 4. From Fig. 8, it can be observed that the negative correlation fitting ability curve of Plackett copula shows a trend of increasing first and then decreasing with the increase of negative correlation. Additionally, the fitting ability reaches the peak near θ=0.15. The fitting ability of

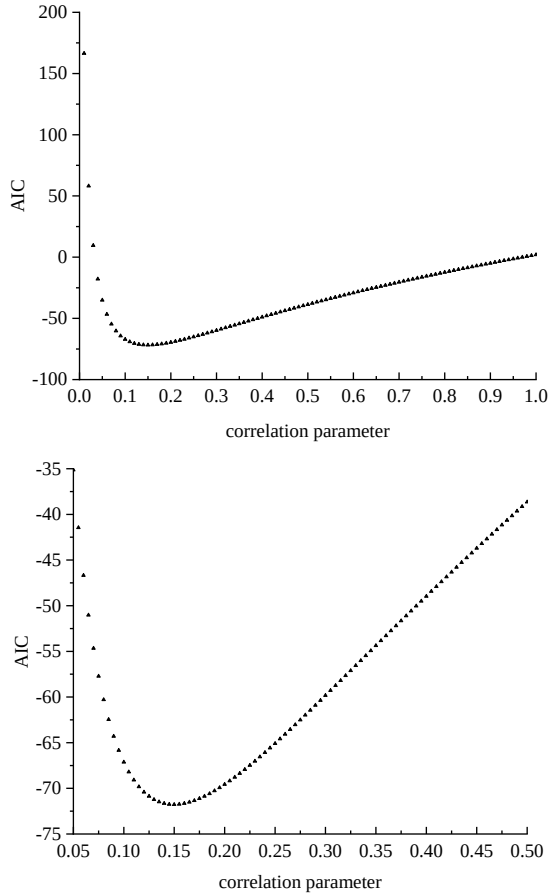

Fig. 8 Plackett copula fitting ability curve with negative correlation. (a) θ from 0 to 1 and (b) θ from 0.05 to 0.5

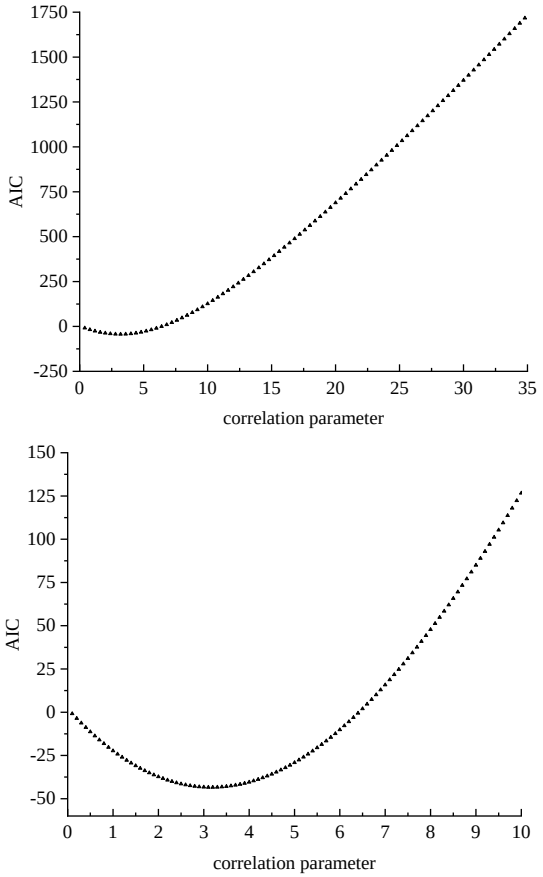

Fig. 9 Frank copula fitting ability curve with positive correlation. (a) θ from 0 to 35 and (b) θ from 0 to 10

Frank copula increases and then decreases with increasing correlation for both positive and negative parameter correlation in Figs. 9 and 10. The optimal fitting ability is near θ=3 and θ=-4.5, respectively. In Fig. 11, the positive correlation fitting ability deformation curve of Clayton copula increases first and then decreases with the increase of positive correlation. When θ is between 0.3 and 0.4, the fitting ability reaches the peak. From Fig. 12, it is evident that the fitting ability of No.16 Copula, which has the superiority in characterizing the negative correlation between parameters, weakens as the negative correlation increases.

Therefore, on account of the positive correlation parameter group in the joint distribution model of geotechnical mechanical parameters, the results obtained from section 3.3.1 show that the fitting effect of Gaussian copula and Frank copula is superior, among which the Gaussian copula correlation parameter is 0.512. Comparing the positive correlation fitting ability curve of Fig. 6, it is at a good level of fitting effect in the whole positive correlation region. When the correlation parameters are close to 1.0, the fitting effect of Gaussian copula will be better; The correlation parameter of Frank copula is 3.29, which is located near the optimal value of the fitting effect. Furthermore, the fitting effect is outstanding. However, the fitting ability will be weaker and weaker by continuously enhancing the positive correlation. Meanwhile, the gap with the fitting ability of Gaussian copula will be further expanded. For Plackett copula, the correlation parameter is 8.863, which is in the weak fitting ability area. When the parameters with stronger correlation are used, the fitting ability will continue to decrease. The worst-fit Clayton copula function is similar to the Plackett copula. As the parameter correlation increases, its fitting ability continues to decrease, and the overall fitting ability is the worst compared to other selected copula functions. For the negative correlation parameter group in the joint distribution model of coal mine geotechnical mechanical parameters, the results obtained from section 3.3.1 reveals that the fitting effects of Gaussian copula, Plackett copula and Frank copula are brilliant. The Gaussian copula correlation parameter is -0.619. When the negative correlation continues to increase, the fitting effect of Gaussian copula will show better fitting ability. The relevant parameters of Plackett copula and Frank copula are near the optimal fitting value, and the fitting effect is great. However, when the negative correlation is strengthened, the fitting ability will be weaker than Gaussian copula; No.16 copula has the worst fitting ability. Moreover, further enhancing the negative correlation will weaken its fitting ability.

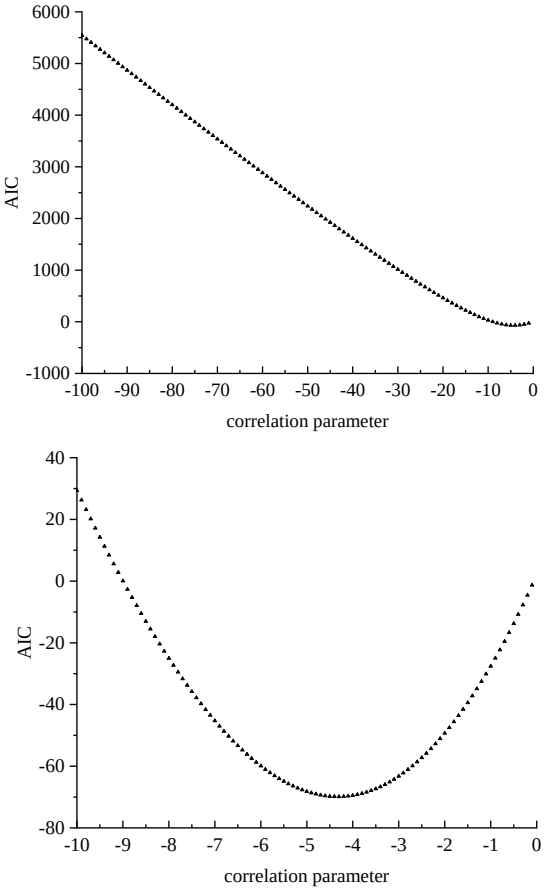

Fig. 10 Frank copula fitting ability curve with negative correlation. (a) θ from -100 to 0 and (b) θ from -10 to 0

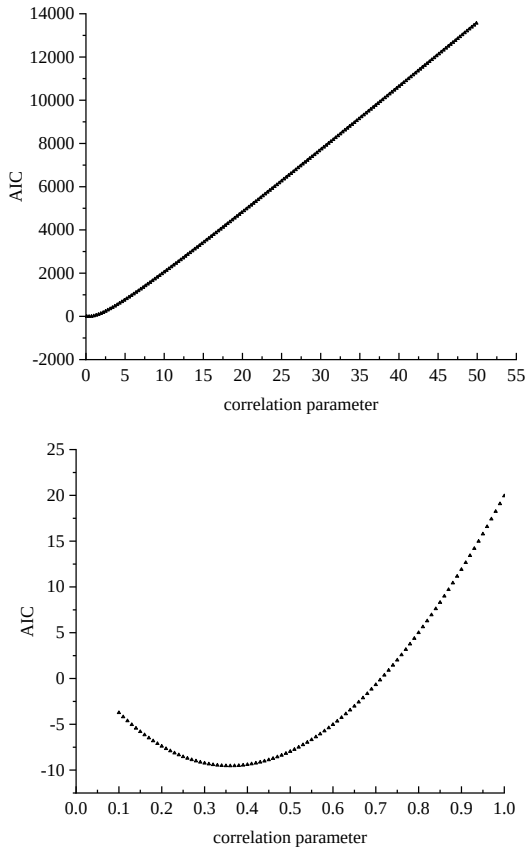

Fig. 11 Clayton copula fitting ability curve with positive correlation. (a) θ from 0 to 50 and (b) θ from 0.1 to 1

4. Conclusions

In this study, a Copula method based on small sample exploration and test data to construct the intensity characteristics of roof geotechnical strata is proposed. Based on 176 sets of measured data of 31 coal mine roofs in China, the goodness of fit and simulation error of the four-dimensional Gaussian Copula constructed using the Pearson method, Kendall method, and Spearman methods are analyzed. The influence of different Copula function structures on the fitting ability of the original data is discussed. The main conclusions are as follows:

(1) The joint probability distribution model can highlight the advantages of the Copula function while independently constructing the marginal distributions of each parameter. When constructing the marginal distributions of parameters, it does not necessarily follow the traditional normal distribution. This provides an effective approach for studying the uncertainty of roof geotechnical parameters.

(2) The simulation effects of different Gaussian Copula construction methods vary, and the Pearson method exhibits better fitting results in constructing correlation parameters. The reason for this may be that when calculating the construction of correlation parameters, all parameters are treated as a unified log-normal distribution, leading to certain inaccuracies.

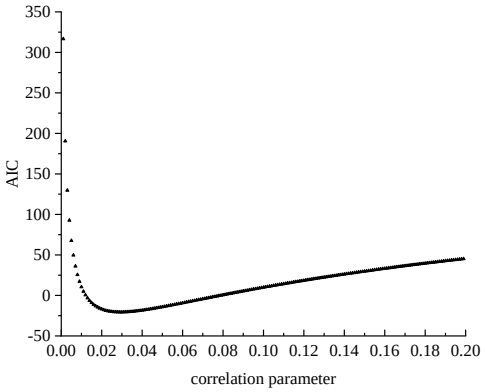

Fig. 12 No.16 copula fitting ability curve with negative correlation

(3) The Kendall rank correlation method and the Spearman rank correlation method have similar simulation errors. In practical use, it is important to be cautious about the uncertainty issue of the Pearson method. Rank correlation methods have the advantages of good universality, good fitting effect, and small variation in simulation errors. In practical engineering applications, rank correlation methods can be given priority consideration.

(4) Gaussian Copula performs well in fitting the correlation structure of commonly used bivariate

parameters, but its errors are relatively small compared to other bivariate Copula functions. In practical engineering applications, it is necessary to verify and assess the correlation structure between parameters in order to select the optimal Copula function that can effectively represent the correlation between parameters.

(5) For the bivariate Copula fitting ability of coal mine geotechnical strength parameters, when the correlation is strong, Gaussian Copula demonstrates the best fitting ability. Other Copula functions that show good fitting effects perform well in the region of fixed correlation parameters. These rules should be taken into account when selecting the optimal Copula after obtaining relevant parameters in practical engineering

Acknowledgements

This research was supported by the National Natural Science Foundation of China (Grant No. 42371133), the Natural Science Foundation of Jiangsu Province of China (Grant No. BK20231501), the Key Research and Development Program of Xuzhou (Grant No. KC23294), the Opening Fund of National Key Laboratory of Petroleum Resources and Engineering, China University of Petroleum, Beijing (Grant No. PRP/open-2211), the Opening Fund of Key Laboratory of Geohazard Prevention of Hilly Mountains, Ministry of Natural Resources (Fujian Key Laboratory Of Geohazard Prevention) (Grant No. FJKLGH2023K003) and the Opening Fund of Technology Innovation Center for Mine Geological Environment Restoration in the Alpine and Arid Regions (Grant No. HHGCKK2205).

Declaration of competing interest

The authors declare that there is no conflict of interest in this study.

References

Akaike, H. (1974), "A new look at the statistic model identification", *IEEE T. Automat. Control*, **19**(6), 716-723

Baecher, G.B. and Christian, J. T. (2003), *Reliability and Statistics in Geotechnical Engineering*. New York: John Wiley and Sons.

Bulent, T. (2017), "Comparison of measurement uncertainty calculation methods on example of indirect tensile strength measurement", *Geomech. Eng.*, **12**(6), 871-882. https://doi.org/10.12989/gae.2017.12.6.871.

Chen, D.X., Sun, C. and Wang, L.G. (2020), "Collapse behavior and control of hard roofs in steeply inclined coal seams", *Bull. Eng. Geol. Environ.*, **80**, 1489-1505. https://doi.org/10.1007/s10064-020-02014-3.

Chen, G.L. (2018), "Research on instability mechanism and pre-stress control technology of coal roadway with composite roof", MA Thesis, Xi'an University of Science and Technology, Xi'an, China. (In Chinese)

Chen, W. (2020), "Study on roof stability of goaf with hard surrounding rock-Take Xinpu Phosphate Mine as an example", MA Thesis, China University of Mining and Technology, Xuzhou, China. (In Chinese)

Cherubini, U., Luciano, E. and Vecchiato, W. (2004), *Copula methods in finance*. John Wiley&Sons, New York.

Chi, X.L. (2021), "Mechanical characteristics of regenerated roof and stability control of surrounding rock in fully-mechanized slicing mining of the soft steeply dipping coal seam", Ph.D.Thesis. Anhui University of Science and Technology, Huainan, China. (In Chinese)

Das, G.K., Hazra, B., Garg, A. and Ng, C.W.W. (2018), "Stochastic hydro-mechanical stability of vegetated slopes: An integrated copula based framework", *Catena*, **160**, 124-133. https://doi.org/10.1016/j.catena.2017.09.009.

Dong, F. (2020), "Stability analysis and governance research on Zhujiaba copper mine", MA Thesis. Kunming University of Science and Technology, Kunming, China. (In Chinese)

Dou, L.T. (2021), "Mechanism and control technology of strong rock pressure induced by structural instability of hard roof in thick coal seam", Ph.D.Thesis. Anhui University of Science and Technology, Huainan, China. (In Chinese)

Embraechts, P., Mcneil, A.J. and Straumann, D. (2002), "Correlation and dependence in risk management: Properties and pitfalls", Dempster M. edited, *Risk Management: Value at Risk and Beyond*, Cambridge University Press. 176-223. https://doi.org/10.1017/ CBO9780511615337.008.

Guo, Y.X. (2016), "Study on stability of tunnel of trickled roof and control technology in Heilongjiang mine", MA Thesis. Taiyuan University of Technology, Taiyuan, China. (In Chinese)

Guo, Y.X. (2019), "Research on stability control technology of the water-sprinkling roof surrounding rock in the water-filled goaf", *Min. Res. Development*, **39**(12), 73-79. (In Chinese)

He, Y.Y. (2020), "Stability and instability process analysis of steep coal seam of No.104 group in Xinjiang", MA Thesis. Xi'an University of Science and Technology, Xi'an, China. (In Chinese)

Hosseini, M., Azhari, A., Lotfi, R. and Baghbanan A. (2023), "Safety analysis of Sormeh underground mine to improve sublevel stoping stability", *Deep Undergr. Sci. Eng.*, **2**(2), 173-187. https://doi.org/10.1002/dug2. 12041.

Huffman, J.C. and Stuedlein, A.W. (2014), "Reliability-based serviceability limit state design of spread footings on aggregate pier reinforced clay", *J. Geotech. Geoenviron. Eng.*, **140**(10), 04014055-04014055. https://doi.org/10.1061/(ASCE)GT.1943-5606.0001156

Jiao, J. (2021), "Research on surrounding rock control technology for roadway driving along goaf of 414110 working face in Shuangxin mining industry", MA Thesis. China University of Mining and Technology, Xuzhou, China. (In Chinese)

Johari, A., Javadi, A.A., Makiabadi, M.H. and Khodaparast, A.R. (2012), "Reliability assessment of liquefaction potential using the jointly distributed random variables method", *Soil Dyn. Earthq. Eng.*, **38**, 81-87. https://doi.org/10.1016/j.soildyn.2012.01.017.

Johari, A., Javadi, A.A., Elmi, M. and Raei, S. (2013), "An analytical approach to reliability assessment of shear wave velocity relationship", *Scientia Iranica*, **20**(6), 1685-1694.

Johari, A., Momeni, M. and Javadi, A.A. (2015), "An analytical solution for reliability assessment of pseudo-static stability of rock slopes using jointly distributed random variables method", *Iranian J. Sci. Tech. T. Civil Eng.*, **39**, 351-363.

Kong, D.Z., Xiong, Y., Cheng, Z.B., Wang, N., Wu, G.Y. and Liu, Y. (2021), "Stability analysis of coal face based on coal face-support-roof system in steeply inclined coal seam", *Geomech. Eng.*, **25**(3), 233-243. https://doi.org/10.12989/gae.2021.25.3.233.

Li, D.Q., Chen, Y.F., Lu, W.B. and Zhou, C.B. (2010), "Stochastic response surface method for reliability analysis of rock slopes involving correlated non-normal variables", *Comput. Geotech.*,

38, 58-68. https://doi.org/10. 1016/j.compgeo.2010.10.006.

Li, Q.Q. (2012), "Feasibility study of naked support on K2 limestone nude under hard roof", MA Thesis. Anhui University of Architecture, Hefei, China. (In Chinese)

Li, Y.L. (2017), "Deformation instability mechanism and supporting technology of large-section coal roadway with layered roof in Zhaozhuang coal mine", Ph.D.Thesis. China University of Mining and Technology(Beijing), Beijing, China. (In Chinese)

Liu, J.X. (2018), "Study on stability mechanism and control of compound roof in coal roadway", MA Thesis. Xi'an University of Science and Technology, Xi'an, China. (In Chinese)

Lukasz, B. and Tadeusz, M. (2020), "An analysis of rock mass characteristics which influence the choice of support", *Geomech. Eng.*, **21**(4), 371-377. https://doi.org/10.12989/gae.2020.21.4.371.

Meng, H. (2018), "Study on stability and controlment of hard roof stope in Qing-dong mine", Ph.D.Thesis. China University of Mining and Technology(Beijing). Beijing, China. (In Chinese)

Meng, Q.B., Kong, L.H., Han, L.J., Li, Y., Nie, J.W., Li, H. and Gao, J. (2017), "Stability control technology for deep soft and broken composite roof in coal roadway", *J. China Coal Soc.*, **42**(10), 2554-2564. (In Chinese)

Minh, C.T. and Jun, H. (2021), "Stochastic vibration analysis of functionally graded beams using artificial neural networks", *Struct. Eng. Mech.*, **78**(5), 529-543. https://doi.org/10.12989/sem.2021.78.5.529.

Nelson, R.B. (2006), *An introduction to copulas*, Springer, New York.

Ng, C.W., Qu, C.X., Cheung, R.W., Guo, H.W., Ni, J.J., Chen, Y.B. and Zhang, S. (2021), "Risk assessment of soil slope failure considering copula-based rotated anisotropy random fields", *Comput. Geotech.*, **136**. https://doi.org/10.1016/j.compgeo.2021.104252.

Niu, X.M. (2013), "Study on roofs' stability of cavities under open-pit mine", MA Thesis. Changsha Mining Research Institute, Changsha, China. (In Chinese)

Palaro, H.P. and Hotta, L.K. (2006), "Using conditional copula to estimate value at risk", *J. Data Sci.*, **4**(1), 93-115. https://doi.org/10.6339/JDS.2006.04(1).226.

Peng, Z.D. (2012), "Ann hill coal roadway roof structure destroy mechanism and its control", MA Thesis. Xi'an University of Science and Technology, Xi'an, China. (In Chinese)

Phoon, K.K., Santoso, A. and Quek, S.T. (2010), "Probabilistic analysis of soil-water characteristic curves", *J. Geotech. Geoenviron. Eng.*, **136**, 445-455. https://doi.org/10.1061/(ASCE)GT.1943- 5606.0000222.

Phoon, K.K. (2020), "The story of statistics in geotechnical engineering", Georisk: *Assessment and Management of Risk for Engineered Systems and Geohazards*, **14**(1), 3-25. https://doi.org/10.1080/17499518.2019.1700423.

Prakash, A., Hazra, B. and Sreedeep, S. (2019), "Probabilistic Analysis of Unsaturated Fly Ash Slope", *J. Hazardous, Toxic, and Radioactive Waste*, **23**(1). https://doi.org/10.1061/(ASCE)HZ.2153-5515.0000428.

Qiu, J.J. (2016), "Research on deformation law and control technology of surrounding rock of large cross section chamber in Shilawusu coal mine", MA Thesis. China University of Mining and Technology, Xuzhou, China. (In Chinese)

Ramanandan, S. and Dodagoudar, G.R. (2020), "Reliability analysis of slopes stabilised with piles using response surface method", *Geomech. Eng.*, **21**(6), 513-525. https://doi.org/10.12989/gae.2020.21.6.513.

Salvadori, G. and Michele, C.D. (2007), "On the use of copulas in hydrology: Theory and practice", *J. Hydrol. Eng.*, **12**(4), 369-380. https://doi.org/10.1061/(ASCE)1084-0699(2007)12:4(369).

Schwarz, G. (1978), "Estimating the dimension of a model", *The Annals of Statistic*, **6**(2), 461-464.

Shang, X.G. (2018), "Study on roof instability mechanism of Datunsong mine goaf based on FLAC3D", MA Thesis. Kunming University of Science and Technology, Kunming, China. (In Chinese)

Shen, F.J. (2015), "The deformation of roof bedding separation critical value of coal mine roadway of 11-2 east Kouzi", MA Thesis. Anhui Jianzhu University, Hefei, China. (In Chinese)

Shen, S.H. (2020), "Research on mechanical properties and it's controlling factors of coal measures rocks in the deep part of Huainan panji mining area", MA Thesis. Anhui University of Science and Technology, Huainan, China. (In Chinese)

Sherizadeh, T. and Kulatilake, P.H. (2016), "Assessment of roof stability in a room and pillar coal mine in the U.S. using three-dimensional distinct element method", *Tunnelling and Underground Space Technology incorporating Trenchless Technology Research*, **59**, 24-37. https://doi.org/10.1016/j.tust.2016.06.005.

Sklar, A. (1959), *Fonctions de repartition a n dimensions et leurs marges.* publ.inst.statist.univ.paris. 8

Soumya, B., Subhasis, C. and Subhasis, D. (2015), "Robust optimization of reinforced concrete folded plate and shell roof structure incorporating parameter uncertainty", *Struct. Eng. Mech.*, **56**(5), 707-726. https://doi.org/10.12989/sem.2015.565.707.

Su, X.G. (2013), "Study on roadway supporting structure and stability coupling control of surrounding rock of extra-thick compound roof", Ph.D.Thesis. Taiyuan University of Technology, Taiyuan, China. (In Chinese)

Sun, J. (2012), "Study on working face movement law and its stability control near fault", MA Thesis. Taiyuan University of Technology, Taiyuan, China. (In Chinese)

Tang, X.S., Wang, M.X. and Li, D.Q. (2020), "Modeling multivariate cross-correlated geotechnical random fields using vine copulas for slope reliability analysis", *Comput. Geotech.*, **127**. https://doi.org/10.1016/j. compgeo. 2020.103784.

Wang, Y.K., Liu, X.L. and Xiong, Y.L. (2022), "Numerical simulation of zonal disintegration of surrounding rock in the deep-buried chamber", *Deep Undergr. Sci. Eng.*, **1**(2), 174-182. https://doi.org/10.1002/dug2. 12017.

Wu, H.T. (2016), "Engineering geological characteristics and stability assessment of No. 4 coal seam's roof in Huangyuchuan coal mine", MA Thesis. Henan Polytechnic University, Jiaozuo, China. (In Chinese)

Wu, X.F. (2022), "Study on stability control technology of roof dripping surrounding rock in Jincheng coal mine", *Shandong Coal Science and Technology*, **40**(7),17-20. (In Chinese)

Yang, C.Z. (2018), "Stability analysis and support technology of surrounding rock of coal roadway with composite roof", *Safety in Coal Mines*, **49**(1), 218-221. (In Chinese)

Yu, Y., Wang, X.Y., Bai, J.B., Zhang, L.Y. and Xia, H.C. (2020), "Deformation mechanism and stability control of roadway surrounding rock with compound roof: Research and applications", *Energies*, **13**(6). https://doi.org/10.3390/en13061350.

Zhang, F.S., Cui, L., An, M.K., Elsworth, D. and He, C.R. (2022), "Frictional stability of Longmaxi shale gouges and its implication for deep seismic potential in the southeastern Sichuan Basin", *Deep Undergr. Sci. Eng.*, **1**(1), 3-14. https://doi.org/10.1002/dug2. 12013.

Zhang, J., Zhang, Y.S., Du, W.Z., Wang, H.W. and Serati, M. (2021), "An analytical approach to estimate the mechanical state of roof strata in underground longwall mining", *Geomech. Eng.*, **27**(1), 55-62. https://doi.org/10.12989/gae. 2021.27.1.057.

Zhang, L. (2010), "Study on failure law and support technique of straticulate roof of hard rock", MA Thesis. Central South University, Changsha, China. (In Chinese)

Zhao, J., Zhang, L. and Wang, S.L. (2021), "Measurement and evolution law of overburden fracture angle in high cutting stope with composite roof", *Coal Eng.*, **3**(1), 75-78. (In Chinese)
Zhao, M.Z. (2020), "Stability mechanism and safety control technology of compound roof in fully mechanized coal roadway of Zhaozhuang mine", Ph.D.Thesis. China University of Mining and Technology (Beijing), Beijing, China. (In Chinese)
Zheng, D.J., Li, X.Q., Yang, M., Su, H.Z. and Gu, C.S. (2018), "Copula entropy and information diffusion theory-basednew prediction method for high dam monitoring", *Earthq. Struct*., **14**(2), 143-153. https://doi.org/10.12989/eas. 2018.14.2.143.
Zhu, P.R. (2019), "Research on caving mechanism and evolution law of roof rock of inclined thick-large ore body by caving method", Ph.D.Thesis. University of Science and Technology Beijing, Beijing, China. (In Chinese)

CC